ACS Medicinal Chemistry Letters

Letter

Class I/IIb-Selective HDAC Inhibitor Exhibits Oral Bioavailability and Therapeutic Efficacy in Acute Myeloid Leukemia

Andrew E. Shouksmith, Justyna M. Gawel, Nabanita Nawar, Diana Sina, Yasir S. Raouf, Shazreh Bukhari, Liying He, Alexandra E. Johns, Pimyupa Manaswiyoungkul, Olasunkanmi O Olaoye, Aaron D. Cabral, Abootaleb Sedighi, Elvin D de Araujo, and Patrick Thomas Gunning

ACS Med. Chem. Lett., **Just Accepted Manuscript** • DOI: 10.1021/acsmedchemlett.9b00471 • Publication Date (Web): 13 Dec 2019

is published by the American Chemical Society. 1155 Sixteenth Street N.W., Washington, DC 20036

Class I/IIb-Selective HDAC Inhibitor Exhibits Oral Bioavailability and Therapeutic Efficacy in Acute Myeloid Leukemia

Andrew E. Shouksmith[†,#], Justyna M. Gawel[†,#], Nabanita Nawar[†], Diana Sina[†], Yasir S. Raouf[†], Shazreh Bukhari[†], Liying He[†], Alexandra E. Johns[†], Pimyupa Manaswiyoungkul[†], Olasunkanmi O. Olaoye[†], Aaron D. Cabral[†], Abootaleb Sedighi[†], Elvin D. de Araujo[†], Patrick T. Gunning[†*]

[†]Department of Chemical and Physical Sciences, University of Toronto Mississauga, 3359 Mississauga Road, Mississauga, Ontario, L5L 1C6, Canada

Abstract

The HDAC inhibitor 4-(*tert*-butyl)-*N*-(4-(hydroxycarbamoyl)phenyl)benzamide (**AES-350**, **51**) was identified as a promising pre-clinical candidate for the treatment of acute myeloid leukemia (AML); an aggressive malignancy with a meagre 24% 5-year survival rate. Through screening of low molecular-weight analogues derived from the previously discovered novel HDAC inhibitor, **AES-135**, compound **51** demonstrated greater HDAC isoform selectivity, higher cytotoxicity in MV4-11 cells, an improved therapeutic window, and more efficient absorption through cellular and lipid membranes. Compound **51** also demonstrated improved oral bioavailability compared to SAHA in mouse models. A broad spectrum of experiments, including FACS, ELISA, and western blotting, were performed to support our hypothesis that **51** dose-dependently triggers apoptosis in AML cells through HDAC inhibition.

Key Words

Histone deacetylases (HDACs), acute myeloid leukemia (AML), enzyme inhibition, pharmacokinetics

Histone acetyltransferases (HATs) and histone deacetylases (HDACs) are two protein classes with antagonistic roles that regulate acetylation of histones as well as various cytoplasmic non-histone proteins.[1,2] HATs catalyze the transfer of acetyl groups to the ε-amino substituent of specific Lys residues, whereas classical HDACs reverse this process using a metal co-factor to catalyze hydrolysis of the acetyl group.[1] There are 18 HDACs in the human proteome grouped into four

classes.[2] Classes I, II, and IV are metal-dependent with corresponding HDAC inhibitors typically coordinating to the metal co-factor rendering the protein inactive. Class III HDACs (sirtuins) operate in conjunction with an NAD^+ co-factor and are not assessed in this study. To date, four small-molecule HDAC inhibitors have received FDA approval for cancer treatment: Vorinostat (SAHA, **1**),[3] Belinostat (PXD101, **2**),[4] Panobinostat (LBH-589, **3**)[5] and Romidepsin (depsipeptide-FK228, **4**)[6] (**Figure 1**). All compounds are approved specifically for hematological malignancies although multiple clinical trials are ongoing with these compounds in combination studies against various cancers, including gliomas, solid tumors, and AML. In contrast to the FDA approved drugs, Ricolinostat and Citarinostat are the first HDAC6 selective inhibitors in clinical trials.[7] HDAC6 is unique among the HDACs in that it is predominantly cytosolic and facilitates microtubule deacetylation as well as regulation of PDL1 and other important targets related to cancer immunotherapy. As such, HDAC6 has been implicated in oncogenesis and metastasis, with the emergence of selective inhibitors as viable cancer therapeutics.[8,9]

Recently, we reported the discovery of **AES-135** (**5**) (**Figure 1**); a novel nanomolar inhibitor of HDAC3, 6, and 11 with *in vitro* cytotoxicity in low passage patient-derived pancreatic cancer cells, even in the presence of cancer-associated fibroblasts (CAFs).[10] Herein, we report efforts to optimize the ligand efficiency of **5** via a focused SAR analysis. Several stripped-down analogues of **5** exhibited enhanced HDAC6 inhibition and selectivity, with one inhibitor (**51**) also demonstrating nanomolar cytotoxicity in MV4-11 (AML) cells.

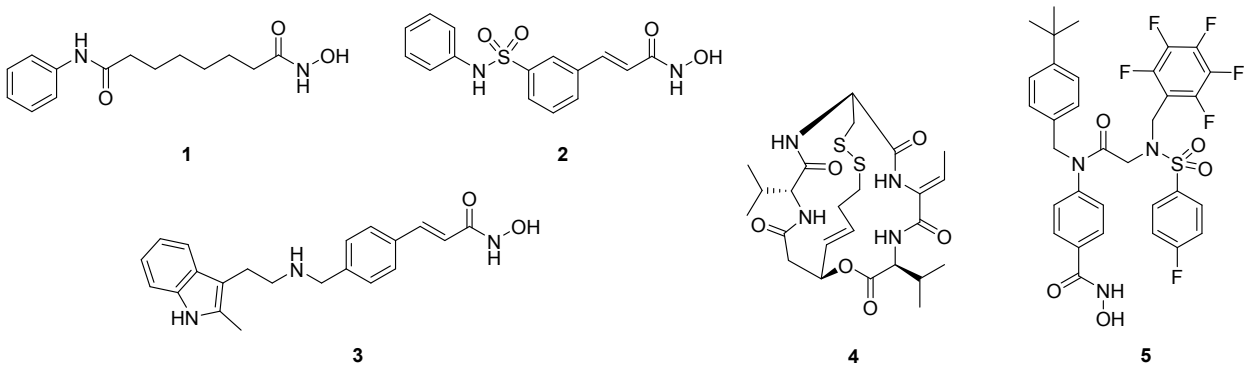

Figure 1: Vorinostat (**1**), Belinostat (**2**), Panobinostat (**3**), Romidepsin (**4**) and **AES-135** (**5**)

Given the molecular weight of **5** (693.7 g/mol), the relative importance of each substituent towards *in vitro* HDAC potency was evaluated through the synthesis of truncated analogues (**35–40**, **46**, **47**, **51**, and **54**). Analogues lacking one substituent were synthesized using **Scheme 1**.

Starting from *tert*-butyl glycine or sarcosine hydrochloride salts (**6–7**), sulfonylation was followed either by acid-mediated removal of the *tert*-butyl protecting group, or by alkylation of the sulfonamide and then *tert*-butyl deprotection to generate carboxylic acids **13–15**. Microwave-assisted coupling with various anilines generated a series of secondary and tertiary amides. Secondary amides were alkylated prior to hydrogenation of the benzyloxy group, and tertiary amides were hydrogenated directly. The resulting carboxylic acids **23–28** were coupled with *O*-benzylhydroxylamine, and hydrogenation of the *O*-benzyl group yielded hydroxamic acids **35–40**.

Scheme 1. Synthesis of compounds **35–40**

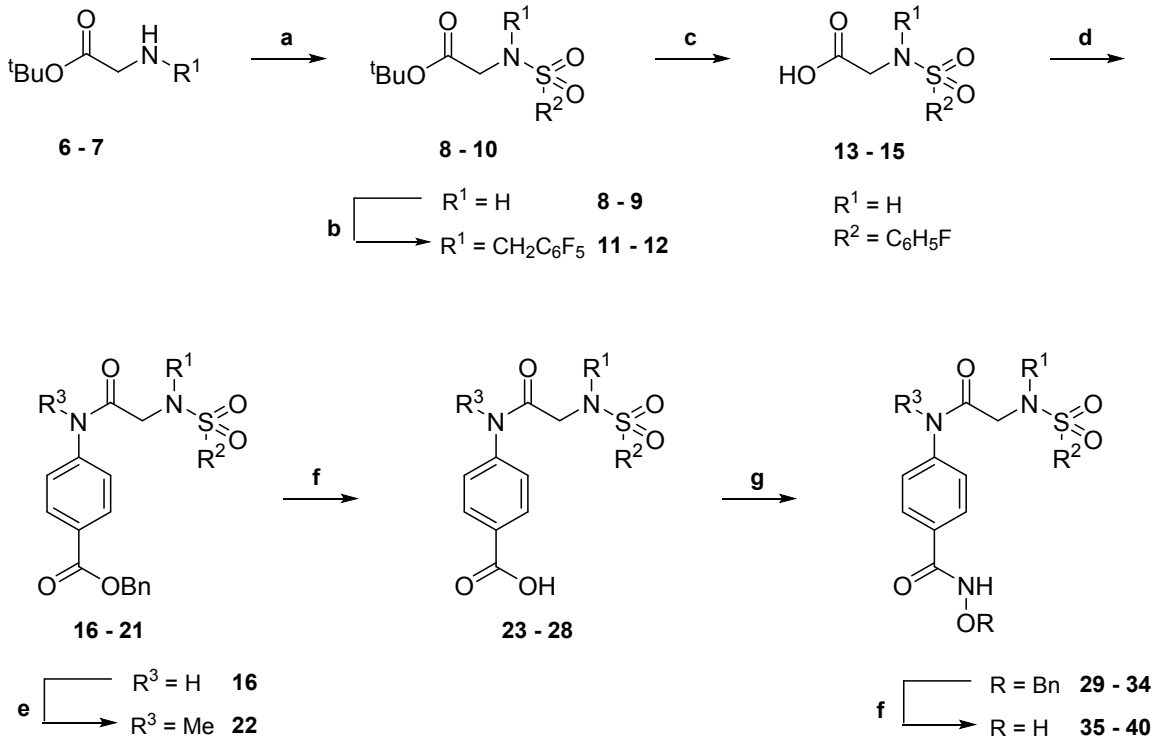

(a) R^2SO_2Cl, $^iPr_2Net$, CH_2Cl_2, 16 h, RT, N_2; (b) Pentafluorobenzyl bromide, Cs_2CO_3, MeCN, 16 h, RT; (c) $CF_3CO_2H/CHCl_3$ (1:3), 24 h, RT; (d) Appropriate aniline, PPh_3Cl_2, $CHCl_3$, 90 min, 100 °C, MW, N_2; (e) MeI, Cs_2CO_3, MeCN, 20 h, RT; (f) H_2, 10% Pd/C, THF/MeOH (2:1), 16 h, RT; (g) (i) $(COCl)_2$, THF, DMF, 2 h, 0 °C; (ii) *O*-benzylhydroxylamine, $^iPr_2NEt$, THF, 16 h, RT, N_2. R^1, R^2, and R^3 are variable depending on the molecule and shown below in Table 1.

Fragment derivatives of **5** lacking the sulfonamide moiety were generated using **Scheme 2**. Reductive amination of benzyl 4-aminobenzoate (**41**) with 4-*tert*-butylbenzaldehyde and protection of the resulting secondary aniline yielded carbamate **43**. Hydrogenation of the

benzyloxy group, coupling with *O*-benzylhydroxylamine, and removal of the *O*-benzyl group generated hydroxamic acid **46**. Subsequent acid-mediated removal of the Boc group yielded compound **47**. Deprotection of the Boc group and acylation of the aniline prior to hydrogenation of the *O*-benzyl group formed compound **54**. Coupling of **10** with 4-*tert*-butylbenzoic acid, followed by conversion of the benzyl ester to the hydroxamic acid, as described previously, gave analogue **51** (**AES-350**).

Scheme 2. Synthesis of compounds **46**, **47**, **51**, and **54**

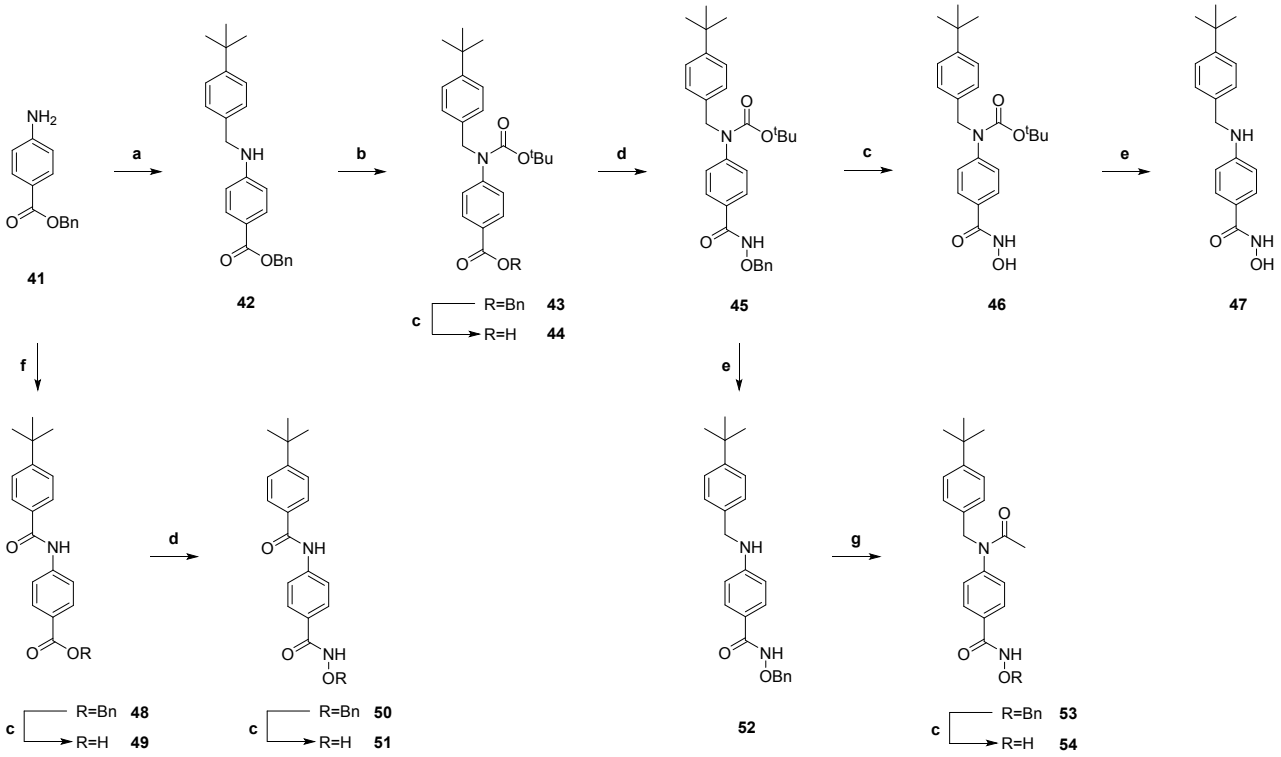

(a) (i) 4-*Tert*-butylbenzaldehyde, THF/TFE (4:1), 16 h, RT; (ii) $NaBH_4$, MeOH, 6 h, RT; (b) $(Boc)_2O$, DMAP, MeCN, 2 h, 80 °C, MW; (c) H_2, 10% Pd/C, THF/MeOH (2:1), 16 h, RT; (d) (i) $(COCl)_2$, THF, DMF, 2 h, 0 °C; (ii) *O*-benzylhydroxylamine, $^iPr_2NEt$, THF, 16 h, RT, N_2; (e) $CF_3CO_2H/CHCl_3$ (1:3), 18 h, RT; (f) 4-*Tert*-butylbenzoic acid, PPh_3Cl_2, $CHCl_3$, 90 min, 100 °C, MW, N_2; (g) AcCl, CH_2Cl_2, 24 h, 0 °C – RT.

All compounds were screened against HDAC3, 6, 8, and 11 in an enzymatic activity assay and fluorescence polarization binding assay. (**Table S2,** Supporting Information). Compounds **35**–**40**, bearing a central amide and lacking one substituent relative to **5**, displayed increased potency against HDAC6 (1.6–128-fold improvement) (**Table 1**). Ostensibly, variations in ligand efficiency altered interactions with other HDAC proteins. Notably, when R^3 is a benzyl substituent (**35**),

general HDAC inhibition increases substantially over the larger *tert*-butylbenzyl or smaller methyl group. When R^1 was changed from a pentafluorobenzene (PFB) (**5**) to a methyl group (**37**) or deleted (**38**), potency against HDACs 3 and 11 was unaffected, but there was a significant gain in HDAC8 potency. Conversion of R^2 from a 4-fluorobenzene (**5**) to a methyl group (**39**) increased HDAC6 and 8 inhibition, but with a concomitant loss in HDAC11 inhibition.

Analogues of **5** with both the PFB and 4-fluorobenzenesulfonamide substituents removed showed high variation in HDAC selectivity (**Table 1**). Boc-protected derivative **46** showed higher potency and selectivity for HDAC6 than **5** or its deprotected derivative **47**. The structurally more rigid amide **51** was similarly potent against HDAC6, but also highly potent against HDAC3 and 8. Acetyl derivative **54** was one of the most potent HDAC8 inhibitors in this series (IC_{50} = 0.085 μM), with comparably high activity against HDAC6 (IC_{50} = 0.071 μM). None of the inhibitors lacking two aromatic substituents from compound **5** showed significant potency against HDAC11, highlighting the importance of steric bulk in the design of HDAC11-targeting compounds.

In conjunction with biochemical assays, inhibitors were assessed for cytotoxic activity in several cancer cell lines including MV4-11 and MOLM-13 (AML), MDA-MB-231 and MDA-MB-468 (breast cancer), as well as MRC-9 lung cells (non-cancerous) and compared to Vorinostat (**1**) and **5** (**Table 1**). Deletion of different substituents resulted in complete abrogation of cytotoxicity in breast cancer cells and reduction in potency in MOLM-13 cells (2–12 fold), with the exception of **39**. In MV4-11 cells, loss of activity was smaller (2–3 fold), with **39** again demonstrating similar potency. While **35** showed impressive HDAC6-selectivity and potency in the enzymatic assay, potency in MV4-11 cells was markedly weaker (>5 μM). Contrastingly, **51** was more potent than **5**, with sub-micromolar activity (IC_{50} = 0.58 ± 0.13 μM) akin to Vorinostat (IC_{50} = 0.31 ± 0.061 μM). At <50% the molecular weight of **5**, compound **51** is more ligand efficient, and exemplifies a large therapeutic index (IC_{50}>30 μM in non-cancerous MRC-9 cells). Compound **51** was also shown to be effective in AML-3 cell lines (IC_{50} = 0.73 ± 0.12 μM) similar to SAHA (IC_{50} = 1.30 ± 0.85 μM) and Citarinostat (IC_{50} = 4.40 ± 0.99 μM). In combination with the observed *in vitro* potency and selectivity of **51** (HDAC6 IC_{50} = 24 nM), it was selected for further pharmacologic studies.

Table 1. IC_{50} values for compounds **35 – 40**, **46**, **47**, **51**, and **54** against HDACs 3, 6, 8, and 11 (EMSA, n = 1) and in MV4-11, MOLM-13, MDA-MB-231, MDA-MB-468, and MRC-9 cells (± SD), and K_i values against zebra-fish HDAC6 catalytic domain 2.

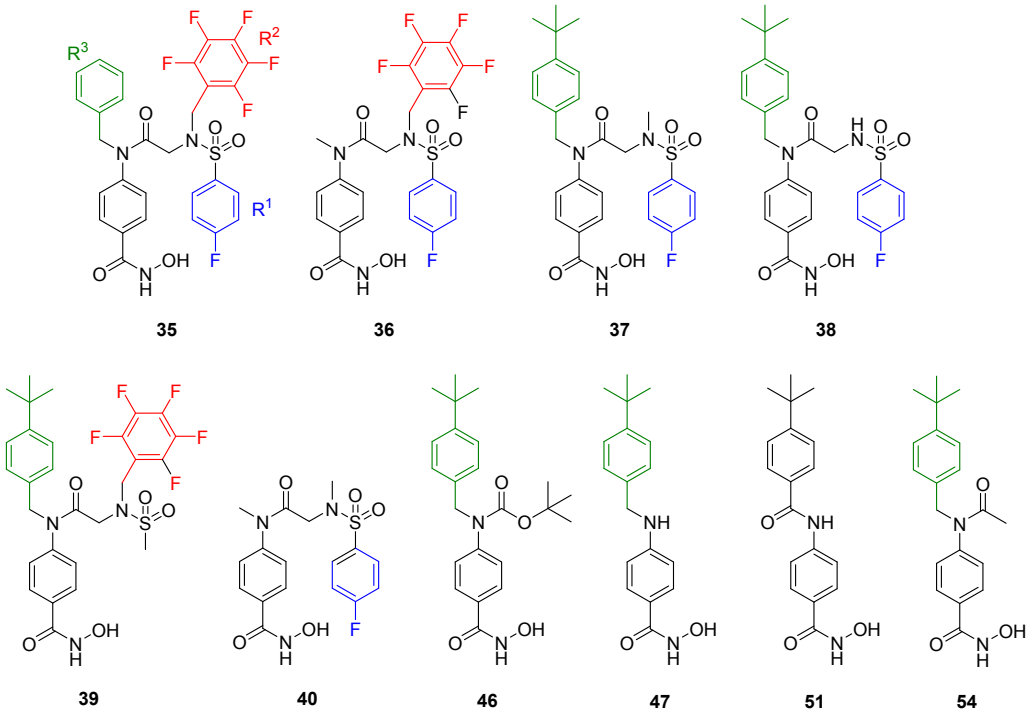

#	HDAC Activity IC_{50} (μM)[a]				HDAC6 K_i (μM)	Cytotoxicity (μM)				
	HDAC3	**HDAC6**	**HDAC8**	**HDAC11**	**HDAC6**	**MV4-11**	**MOLM-13**	**MDA-MB-231**	**MDA-MB-468**	**MRC-9**
1	0.00657	0.0058	0.497	>1	<0.035	0.310 ± 0.061[c]	0.345 ± 0.035[b]	-	-	>25[b]
5	0.654	0.190	>1	0.636	3.600	1.88 ± 0.89[d]	2.10 ± 0.22[c]	2.62 ± 0.56[c]	4.21 ± 1.76[d]	19.2 ± 5.80[c]
35	0.132	0.00149	0.0906	0.0519	1.860	5.80 ± 1.37[b]	8.05 ± 1.31[b]	-	-	-
36	0.213	0.0201	0.224	>1	0.573	3.24 ± 1.14[b]	14.1 ± 4.56[b]	>25[b]	>25[b]	>25[b]
37	0.492	0.0552	0.0379	0.697	0.768	3.41 ± 0.29[b]	5.46 ± 0.74[b]	>25[b]	>12.5[b]	11.8 ± 1.46[b]
38	0.372	0.0528	0.0280	0.665	0.293	3.33 ± 0.34[b]	5.11 ± 0.88[b]	-	>12.5[b]	10.8 ± 0.45[b]
39	0.213	0.0277	0.133	>1	1.093	1.62 ± 0.29[c]	2.98 ± 0.36[b]	>12.5[b]	>25[b]	>25[b]
40	0.708	0.117	0.573	>1	0.793	14.6 ± 1.44[b]	24.8 ± 1.30[b]	-	-	-
46	0.374	0.0282	0.635	0.837	0.201	3.12 ± 0.66[b]	10.3 ± 0.95[b]	>25[b]	>25[b]	9.49 ± 0.57[b]

47	0.503	0.110	>1	>1	0.451	3.49 ± 1.06[b]	9.47 ± 2.12[b]	>25[b]	>25[b]	16.1 ± 0.34[b]
51	0.187	0.0244	0.245	>1	0.035	0.576 ± 0.131[e]	6.00 ± 2.74[c]	>25[b]	>50[b]	33.2 ± 10.3[b]
54	0.276	0.0713	0.0854	>1	0.199	4.24 ± 2.83[b]	10.6 ± 2.17[b]	>25[b]	>25[b]	-

[a]Compounds evaluated to 1 μM; [b]n = 2; [c]n = 3; [d]n = 4; [e]n = 8; R^1, R^2, R^3 shown in blue, red, and green respectively.

The cytotoxicity data for **51** was corroborated by fluorescence-activated cell sorting (FACS) (**Figure 2**). MV4-11 cells were cultured for 18 h with increasing concentrations of **51** or SAHA, before treatment with apoptosis indicators Annexin V and propidium iodide. The findings revealed a clear dose-dependent increase with the percentage of cells entering late-stage apoptosis, similar to SAHA, further supporting the anticancer activity of **51** in this cell line. *In vitro* stability of **51** was evaluated in mouse hepatocytes, by comparing the rates of intrinsic clearance of Verapamil (control) with **51**. Compound **51** ($t_{½}$ = 28.3 min) exhibited ~1.5-fold longer half life than Verapamil ($t_{½}$ = 18.0 min). Previous assays under the same conditions revealed a longer half-life for **5** ($t_{½}$ = 38.5 min), although Verapamil also showed a 17.8% variation ($t_{½}$ = 21.9 min).[10] Normalizing the data of **5** and **51** according to the control Verapamil, suggests that after removing >50% of the total mass of **5**, the hepatocyte half-life of **51** was reduced by only 10%. Similarly, the clearance rate of **51** (49.1 μL/min per 10^6 cells) was lower than that of Verapamil (77.0 μL/min per 10^6 cells) but faster than **5** (36.0 μL/min per 10^6 cells) (**Table S5, Figures S12 – S15,** Supporting Information).

A.

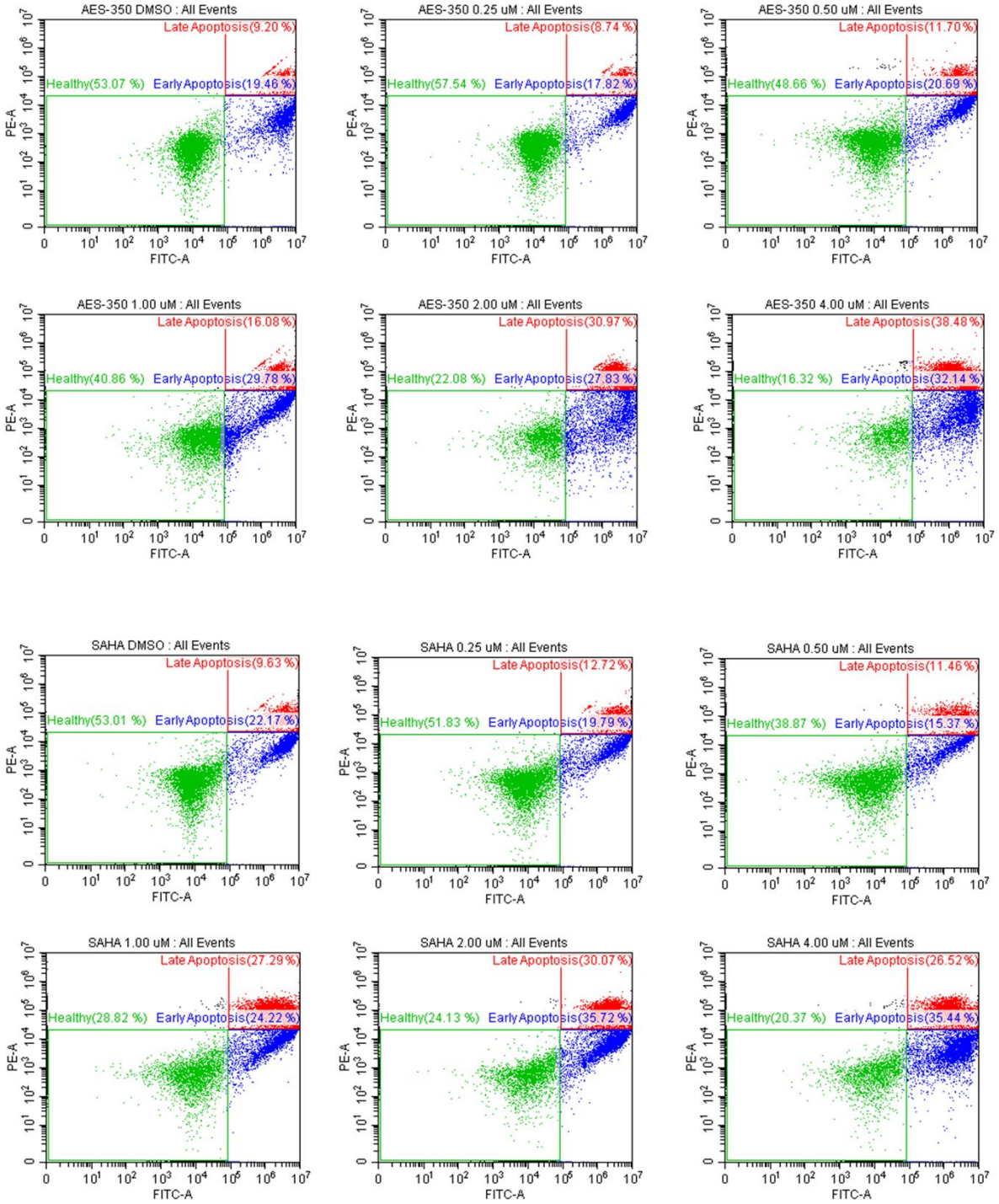
AES-350 DMSO : All Events
Late Apoptosis(9.20 %)
Healthy(53.07 %)
Early Apoptosis(19.46 %)
AES-350 0.25 uM : All Events
Late Apoptosis(8.74 %)
Healthy(57.54 %)
Early Apoptosis(17.82 %)
AES-350 0.50 uM : All Events
Late Apoptosis(11.70 %)
Healthy(48.66 %)
Early Apoptosis(20.69 %)
AES-350 1.00 uM : All Events
Late Apoptosis(16.08 %)
Healthy(40.86 %)
Early Apoptosis(29.78 %)
AES-350 2.00 uM : All Events
Late Apoptosis(30.97 %)
Healthy(22.08 %)
Early Apoptosis(27.83 %)
AES-350 4.00 uM : All Events
Late Apoptosis(38.48 %)
Healthy(16.32 %)
Early Apoptosis(32.14 %)
SAHA DMSO : All Events
Late Apoptosis(9.63 %)
Healthy(53.01 %)
Early Apoptosis(22.17 %)
SAHA 0.25 uM : All Events
Late Apoptosis(12.72 %)
Healthy(51.83 %)
Early Apoptosis(19.79 %)
SAHA 0.50 uM : All Events
Late Apoptosis(11.46 %)
Healthy(38.87 %)
Early Apoptosis(15.37 %)
SAHA 1.00 uM : All Events
Late Apoptosis(27.29 %)
Healthy(28.82 %)
Early Apoptosis(24.22 %)
SAHA 2.00 uM : All Events
Late Apoptosis(30.07 %)
Healthy(24.13 %)
Early Apoptosis(35.72 %)
SAHA 4.00 uM : All Events
Late Apoptosis(26.52 %)
Healthy(20.37 %)
Early Apoptosis(35.44 %)
PE-A
FITC-A

B.

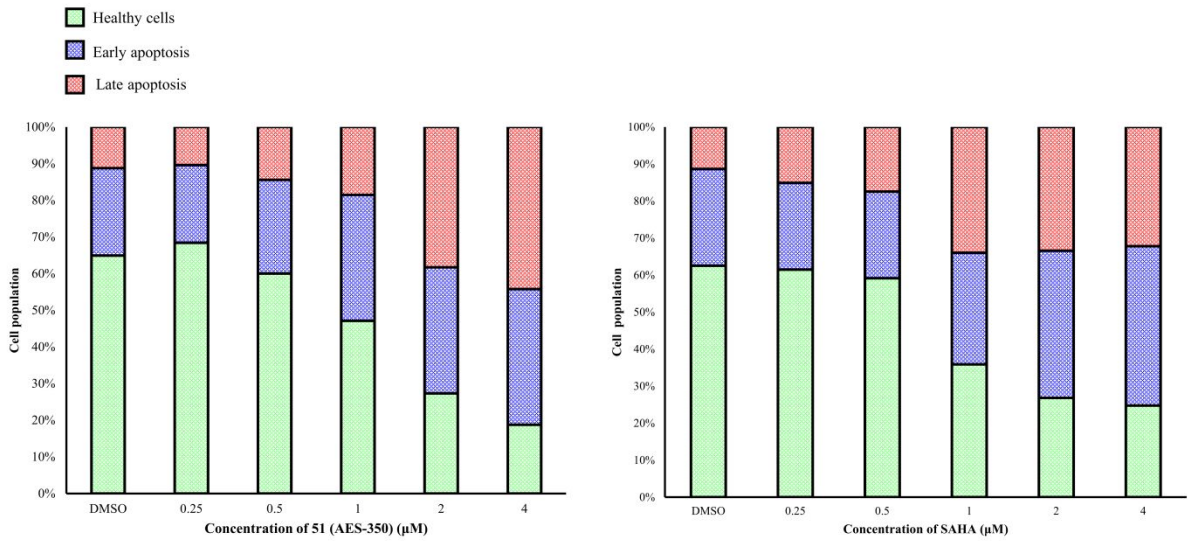

Figure 2: (A) Dot plots and (B) stacked bar graphs representing the distribution of MV4-11 cells classed as healthy, early apoptosis, and late apoptosis 18 h post-dosing with varying concentrations of SAHA and **51** (AES-350) using FACs.

Notably, **51** is markedly less bound to plasma proteins (95.3% protein bound) compared to **5** (99.6%), although both compounds were poorly recovered (~20%) suggesting a metabolic liability in their composition. (**Tables S6 – S8,** Supporting Information).[10]

The significantly lower molecular weight of **51** (312.4 g/mol) suggests it would exhibit superior membrane permeability in comparison to **5**. Parallel artificial membrane permeability assay (PAMPA) was used to approximate permeation of **51** through the blood-brain barrier, where a permeability coefficient (-Log P_e) <6 is defined as having high permeability. Compound **51** was found to have a -Log P_e of 5.14, indicating relatively good lipid bilayer permeability, and was 87.1% recovered in comparison to the parent **5** (-Log P_e = 7.73, 28.7 % recovery, **Tables S9–S12,** Supporting Information). **51** was further analyzed in a small intestinal membrane model (Caco-2) assay to gauge permeability through a monolayer of epithelial cells as well as compound efflux. Metoprolol and Digoxin were used as controls with low and high efflux ratios respectively. In agreement with PAMPA, **51** demonstrated a high permeability (apparent permeability coefficient, P_{app} A-B = 3.45 × 10^{-6} cm/s), approximately 13-times the rate of **5** (P_{app} A-B = 0.27 × 10^{-6} cm/s), Additionally, efflux ratios for Metoprolol, Digoxin and **5** were all higher (1.00, 72.99 and 3.83, respectively) in comparison to **51** (0.64) indicating that **51** would likely demonstrate intestinal absorption if ingested orally (**Tables S13 – S17,** Supporting Information).[11]

To gain a comprehensive HDAC selectivity profile of **51,** the compound was screened *in vitro* against all 11 metal-dependent HDACs (**Table 2**). Known pan-HDAC inhibitors Trichostatin A (TSA), Quisinostat (JNJ-26481585, Phase II clinical trials in CTCL and ovarian cancer), and Group I-selective inhibitor Entinostat (MS-275, Phase III clinical trials in breast cancer / Phase II trials in renal cell carcinoma) were used as positive controls and showed IC_{50} values/selectivity profiles consistent with the literature.[12–14] **51** was found to be selective for HDAC6 with no inhibition observed for the remaining HDACs at >1 μM, in contrast to both Quisinostat and Entinostat which displayed low nM IC_{50} values against almost all HDACs (**Tables S2–S4**, **Figures S1–S11,** Supporting Information). Indeed, **51** could be considered equally to marginally more selective for HDAC6 than Ricolinostat and Citarinostat under these assay conditions. Although both compounds are more potent than **51** against HDAC6, they are also more potent against HDAC3, which reduces their selectivity.

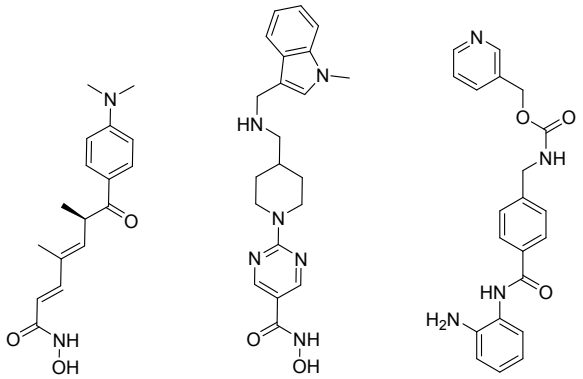

Table 2. IC_{50} Values for **51** Against 11 Classical HDACs (EMSA, n = 1)

	HDAC IC_{50} (μM)[a]										
Cpd	**1**	**2**	**3**	**4**	**5**	**6**	**7**	**8**	**9**	**10**	**11**
51	0.605	>1	0.187	>1	>1	0.0244	>1	0.245	>1	0.899	>1
TSA	0.000681	0.00274	0.000404	>1	0.776	0.000954	0.482	0.207	>1	0.00161	>1
JNJ-26481585	0.000617	0.00216	0.000478	0.00461	0.00595	0.0399	0.00404	0.0024	0.0067	0.00196	>1

MS-275	0.118	0.247	0.223	>1	>1	>1	>1	>1	>1	>1	>1
Ricolinostat	-	0.379	0.0143	>1	-	0.00259	-	0.245	-	-	>1
Citarinostat	-	0.318	0.0125	>1	-	0.00221	-	0.171	-	-	>1

To explain the observed selectivity of **51**, the compound was modelled in the catalytic domain 2 (CD2) of HDAC6 and HDAC8 using Maestro v11.9.01 (Schrödinger, LLC, New York, NY 2019).[15–17] (**Figure 3A–D**) The hydroxamic acid of **51** formed a H-bond between the carbonyl oxygen and hydroxyl group of Tyr745 (HDAC6) or Tyr306 (HDAC8), and a salt bridge interaction between the deprotonated acid and protonated His573 (HDAC6) or His142 (HDAC8). Crucially, the benzene ring of **51** formed π-stacking interactions with Phe583 and Phe643 of HDAC6 not observed in HDAC8. This twin π-stacking phenomenon is responsible for selectivity of this structural motif for HDAC6 over other isoforms.[18,19] Additionally, the amide NH in **51** formed a hydrogen bond with the hydroxyl of Ser531, giving an average free energy of binding (ΔG_B) of -8.5 kcal/mol. Neither of these interactions were observed with HDAC8 (ΔG_B was -7.8 kcal/mol, **Figure S16,** Supporting Information).

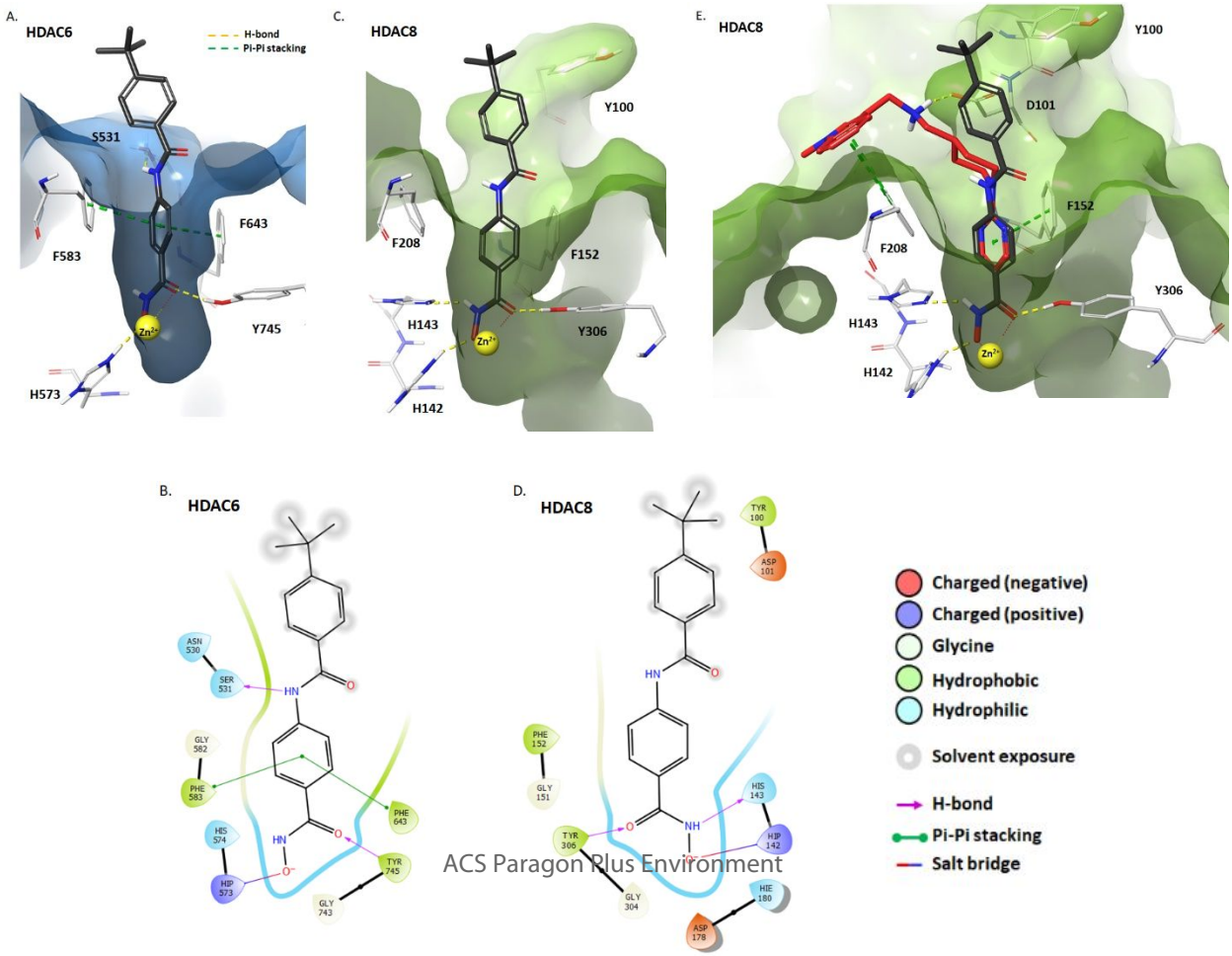

Figure 3: A. Docking of **51** with zebra fish HDAC6 CD2 (light blue) (PDB: 6CSR), **B.** Ligand interaction diagram depicting the key interactions of **51** in HDAC6 CD2. **C.** Docking of **51** in the human HDAC8 catalytic domain (green) (PDB: 6HSK). **D.** Ligand interaction diagram depicting the key interactions of **51** in the HDAC8 catalytic domain. **E.** Overlap of **51** (grey) with Quisinostat (red) in the human HDAC8 catalytic domain (PDB: 6HSK). In A, C, and E, **51** is illustrated by grey (C), white (H), blue (N), red (O), yellow (Zn^{2+}). Other interactions are shown as follows: π-stacking (green dashed lines), H-bonds and salt bridges (yellow dashed lines) and Zn^{2+} chelation (yellow/red dots).

To validate the proposed cellular HDAC inhibition, an enzyme-linked immunosorbent-based assay (ELISA) was performed using HeLa cervical cancer cell lysates. HeLa cells highly express HDAC6, and were sensitive to **51** (IC_{50} = 2.53 ± 0.57 μM) (**Table S1,** Supporting Information). Correspondingly, ELISA-assays depicted a dose-dependent increase in HDAC6 inhibition (IC_{50} = 0.58 μM), and supported **51**-induced cell death via HDAC6 inhibition (**Figure 4A**). ELISA-based data were also supported by western blot analysis of **51**-treated MV4-11 cells (**Figure 4B**) with a dose-dependent increase in acetylated alpha-tubulin (Ac-α-tubulin), a substrate of HDAC6.[20] Collectively, ELISA and western blot analysis suggest **51** elicits HDAC6 inhibition *in vitro* to dose-dependently facilitate apoptosis. It is important to note that despite the observed HDAC6 selectivity *in vitro* there is also a significant reduction of the biomarker of acetylated histone (Ac-Histone H3, which is a biomarker of pan-HDAC activity),[21] and acetylated tubulin *in cellulo* which suggests there may be additional Class I activity of the compound.[9] As such, the *in vitro* selectivity of **51** may not be observed *in cellulo* to same extent which may be the result of alternative inhibition mechanisms.

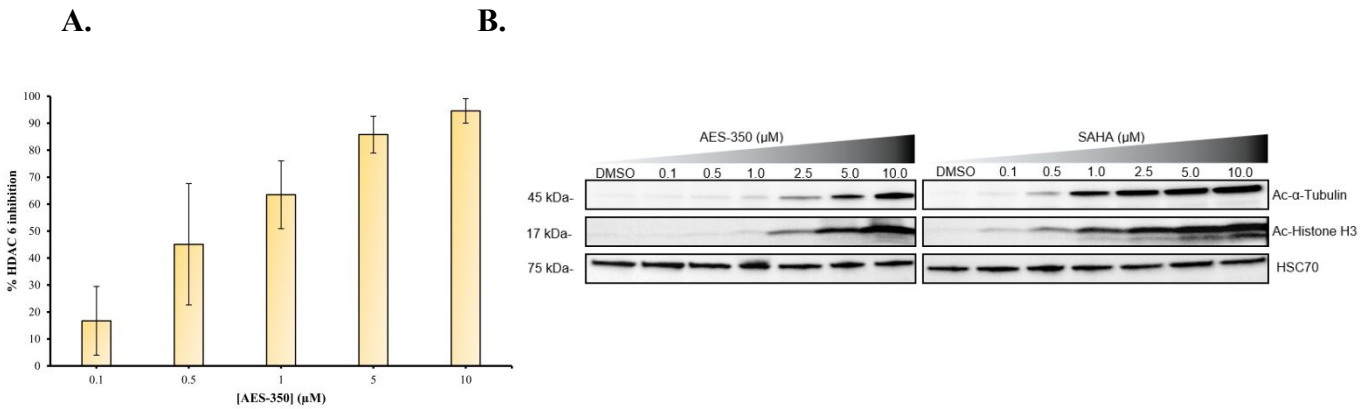

Figure 4: A. HDAC6 inhibition profile with varying concentrations of **51** in HeLa cell lysates (IC_{50} = 0.58 ± 0.13 μM, *n* = 2). **B.** Western blots probing for Ac-α-tubulin, Ac-Histone H3, and HSC70 from MV4-11 after 6 h with varying concentrations of **51** and SAHA.

To evaluate pharmacokinetic (PK) properties of **51**, CD-1 mice were dosed (20 mg/Kg, PO, and 5 mg/Kg IV; **Figure 5**, **Table S18 – S22,** Supporting Information). The single dose oral bioavailability (F) of **51** was 19.8%. In comparison, the reported F value for SAHA in mice is significantly lower (8%).[22] The rapid clearance rate of **51** would require regular dosing, alternative administration routes, or larger dosages. In previous studies, **5** achieved an average C_{max} of 10.74 μM in NSG mice that was sustained for 8 h ($t_{½}$ = 5.0 h).[10] However, it should be noted that **5** could only be dosed by IP, due to poor absorption profiles.

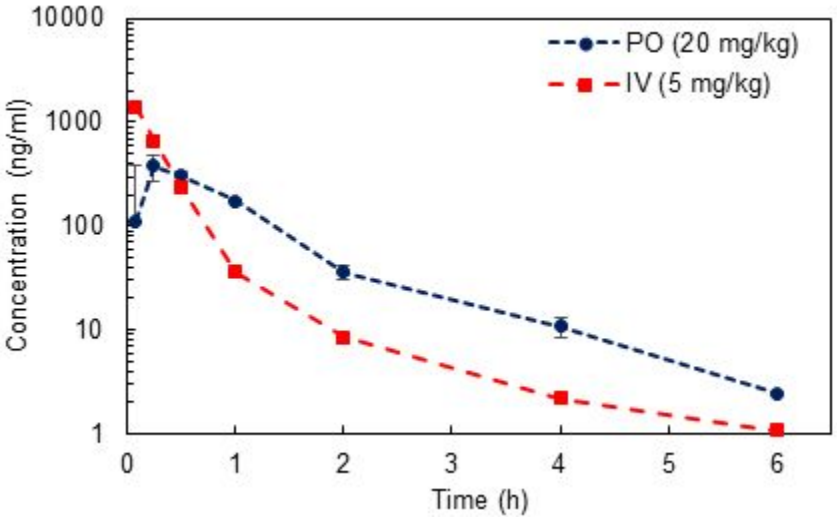

Figure 5. Mean Plasma Concentrations of **51** in CD-1 Mice Following PO (20 mg/Kg, *n* = 3) and IV administration (5 mg/Kg, *n* = 3)

Systematic modifications of novel HDAC inhibitor, **5**, led to the discovery of **51**, a comparatively ligand-efficient compound. Encouragingly, **51**, exhibited an *in vitro* HDAC6 selectivity profile comparable to that of Ricolinostat and Citarinostat. This translated into cellular target engagement, with dose-dependent HDAC6 inhibition in HeLa and MV4-11 cells. Although **51** did not display the same extent of HDAC6 selectivity *in cellulo* as observed in the *in vitro* studies, the compound demonstrated superior cytotoxicity compared to its predecessor in MV4-11, which was corroborated with FACS experiments. The membrane permeability of **51** was also significantly improved compared to **5** based on PAMPA and Caco-2 assays, which translated into

an orally absorbed therapeutic in CD-1 mice. While initial pharmacological data have been promising, ultimately, **51** was not as potent as its FDA-approved competitor SAHA in AML cells. Moreover, although **51** was discovered during our SAR studies, we subsequently discovered it had been previously documented in patent literature.[23–25] Despite these shortcomings, this investigation represents the first disclosure of the mechanism of action for **51** in cancer cells with potency for AML, potentially enabling close analogues to reach pre-clinical investigation for AML treatment. Overall, **51** represents an improved orally bioavailable analogue of **5**, and a promising candidate for further medicinal chemistry efforts to build upon the HDAC selectivity/potency and pharmacological properties.

Supporting Information

- Details of compound synthesis, characterization, *in vitro*, and *in cellulo* assays
- Molecular formula strings for final compounds

Author Information:

Author Addresses:

Department of Chemical and Physical Sciences, University of Toronto Mississauga, 3359 Mississauga Rd N., Mississauga, Ontario L5L 1C6, Canada

*E-mail: patrick.gunning@utoronto.ca. Telephone: (905) 828-5354.

Author Contributions:

[#]A.E.S and J.M.G contributed equally to this work. A.E.S., J.M.G., L.H., A.E.J., A.D.C synthesized/characterized the compounds. J.M.G., N.N., D.S., S.B., P.M., O.O.O., E.D.A., A.S. carried out biological and biophysical evaluation of the compounds. Y.S.R. performed *in silico* experiments. A.E.S., J.M.G., E.D.A., and P.T.G. wrote the manuscript with input from all authors.

Acknowledgements:

P.T.G is supported by research grants from NSERC (RGPIN-2014-05767), CIHR (MOP-130424, MOP-137036), Canada Research Chair (950-232042), Canadian Cancer Society (703963), Canadian Breast Cancer Foundation (705456), Leukemia and Lymphoma Society of Canada and

infrastructure grants from CFI (33536) and the Ontario Research Fund (34876). A.E.S. is supported by a Mitacs Accelerate Grant (IT05960).

Abbreviations used:

HAT, histone acetyltransferase; HDAC, histone deacetylase; SAHA, suberanilohydroxamic acid; CTCL, cutaneous T-cell lymphoma; PTCL, peripheral T-cell lymphoma; MM, multiple myeloma; AML, acute myeloid leukemia; CAF, cancer-associated fibroblast; IP, intraperitoneal; PO, *per os*; Boc, *tert*-butoxycarbonyl; PFB, pentafluorobenzyl; FB, fluorobenzene; EMSA, electrophoretic mobility shift assay; FACS, fluorescence-activated cell sorting; ELISA, enzyme-linked immunosorbent assay; PAMPA, parallel artificial membrane permeability assay; TSA, trichostatin A;

References:

(1) Khan, O.; La Thangue, N. B. HDAC Inhibitors in Cancer Biology: Emerging Mechanisms and Clinical Applications. *Immunology and Cell Biology*. 2012, pp 85–94. https://doi.org/10.1038/icb.2011.100.

(2) Ceccacci, E.; Minucci, S. Inhibition of Histone Deacetylases in Cancer Therapy: Lessons from Leukaemia. *British Journal of Cancer* **2016**, *114* (6), 605–611. https://doi.org/10.1038/bjc.2016.36.

(3) Kumagai, T.; Wakimoto, N.; Yin, D.; Gery, S.; Kawamata, N.; Takai, N.; Komatsu, N.; Chumakov, A.; Imai, Y.; Koeffler, H. P. Histone Deacetylase Inhibitor, Suberoylanilide Hydroxamic Acid (Vorinostat, SAHA) Profoundly Inhibits the Growth of Human Pancreatic Cancer Cells. *International Journal of Cancer* **2007**, *121* (3), 656–665. https://doi.org/10.1002/ijc.22558.

(4) Qian, X.; Ara, G.; Mills, E.; LaRochelle, W. J.; Lichenstein, H. S.; Jeffers, M. Activity of the Histone Deacetylase Inhibitor Belinostat (PXD101) in Preclinical Models of Prostate Cancer. *International Journal of Cancer* **2008**, *122* (6), 1400–1410. https://doi.org/10.1002/ijc.23243.

(5) Ellis, L.; Pan, Y.; Smyth, G. K.; George, D. J.; McCormack, C.; Williams-Truax, R.; Mita,

M.; Beck, J.; Burris, H.; Ryan, G.; et al. Histone Deacetylase Inhibitor Panobinostat Induces Clinical Responses with Associated Alterations in Gene Expression Profiles in Cutaneous T-Cell Lymphoma. *Clinical Cancer Research* **2008**, *14* (14), 4500–4510. https://doi.org/10.1158/1078-0432.CCR-07-4262.

(6) Piekarz, R. L.; Frye, R.; Turner, M.; Wright, J. J.; Allen, S. L.; Kirschbaum, M. H.; Zain, J.; Prince, H. M.; Leonard, J. P.; Geskin, L. J.; et al. Phase II Multi-Institutional Trial of the Histone Deacetylase Inhibitor Romidepsin as Monotherapy for Patients with Cutaneous T-Cell Lymphoma. *Journal of Clinical Oncology* **2009**, *27* (32), 5410–5417. https://doi.org/10.1200/JCO.2008.21.6150.

(7) Dasmahapatra, G.; Patel, H.; Friedberg, J.; Quayle, S. N.; Jones, S. S.; Grant, S. In Vitro and in Vivo Interactions between the HDAC6 Inhibitor Ricolinostat (ACY1215) and the Irreversible Proteasome Inhibitor Carfilzomib in Non-Hodgkin Lymphoma Cells. *Molecular Cancer Therapeutics* **2014**, *13* (12), 2886–2897. https://doi.org/10.1158/1535-7163.MCT-14-0220.

(8) Li, T.; Zhang, C.; Hassan, S.; Liu, X.; Song, F.; Chen, K.; Zhang, W.; Yang, J. Histone Deacetylase 6 in Cancer. *Journal of Hematology and Oncology*. 2018. https://doi.org/10.1186/s13045-018-0654-9.

(9) Vogl, D. T.; Raje, N.; Jagannath, S.; Richardson, P.; Hari, P.; Orlowski, R.; Supko, J. G.; Tamang, D.; Yang, M.; Jones, S. S.; et al. Ricolinostat, the First Selective Histone Deacetylase 6 Inhibitor, in Combination with Bortezomib and Dexamethasone for Relapsed or Refractory Multiple Myeloma. *Clinical Cancer Research* **2017**, *23* (13), 3307–3315. https://doi.org/10.1158/1078-0432.CCR-16-2526.

(10) Shouksmith, A. E.; Shah, F.; Grimard, M. L.; Gawel, J. M.; Raouf, Y. S.; Geletu, M.; Berger-Becvar, A.; De Araujo, E. D.; Luchman, H. A.; Heaton, W. L.; et al. Identification and Characterization of AES-135, a Hydroxamic Acid-Based HDAC Inhibitor That Prolongs Survival in an Orthotopic Mouse Model of Pancreatic Cancer. *Journal of Medicinal Chemistry* **2019**, *62* (5), 2651–2665. https://doi.org/10.1021/acs.jmedchem.8b01957.

(11) Sambuy, Y.; De Angelis, I.; Ranaldi, G.; Scarino, M. L.; Stammati, A.; Zucco, F. The

Caco-2 Cell Line as a Model of the Intestinal Barrier: Influence of Cell and Culture-Related Factors on Caco-2 Cell Functional Characteristics. *Cell Biology and Toxicology*. 2005, pp 1–26. https://doi.org/10.1007/s10565-005-0085-6.

(12) Tong, W. G.; Wei, Y.; Stevenson, W.; Kuang, S. Q.; Fang, Z.; Zhang, M.; Arts, J.; Garcia-Manero, G. Preclinical Antileukemia Activity of JNJ-26481585, a Potent Second-Generation Histone Deacetylase Inhibitor. *Leukemia Research* **2010**, *34* (2), 221–228. https://doi.org/10.1016/j.leukres.2009.07.024.

(13) Arts, J.; King, P.; Mariën, A.; Floren, W.; Beliën, A.; Janssen, L.; Pilatte, I.; Roux, B.; Decrane, L.; Gilissen, R.; et al. JNJ-26481585, a Novel "Second-Generation" Oral Histone Deacetylase Inhibitor, Shows Broad-Spectrum Preclinical Antitumoral Activity. *Clinical Cancer Research* **2009**, *15* (22), 6841–6851. https://doi.org/10.1158/1078-0432.CCR-09-0547.

(14) Tatamiya, T.; Saito, A.; Sugawara, T.; Nakanichi, O. Isozyme-Selective Activity of the HDAC. In *Proc Amer Assoc Cancer Res*; 2004; Vol. 2004, pp 5–6.

(15) Friesner, R. A.; Murphy, R. B.; Repasky, M. P.; Frye, L. L.; Greenwood, J. R.; Halgren, T. A.; Sanschagrin, P. C.; Mainz, D. T. Extra Precision Glide: Docking and Scoring Incorporating a Model of Hydrophobic Enclosure for Protein-Ligand Complexes. *Journal of Medicinal Chemistry* **2006**, *49* (21), 6177–6196. https://doi.org/10.1021/jm051256o.

(16) Halgren, T. A.; Murphy, R. B.; Friesner, R. A.; Beard, H. S.; Frye, L. L.; Pollard, W. T.; Banks, J. L. Glide: A New Approach for Rapid, Accurate Docking and Scoring. 2. Enrichment Factors in Database Screening. *Journal of Medicinal Chemistry* **2004**, *47* (7), 1750–1759. https://doi.org/10.1021/jm030644s.

(17) Friesner, R. A.; Banks, J. L.; Murphy, R. B.; Halgren, T. A.; Klicic, J. J.; Mainz, D. T.; Repasky, M. P.; Knoll, E. H.; Shelley, M.; Perry, J. K.; et al. Glide: A New Approach for Rapid, Accurate Docking and Scoring. 1. Method and Assessment of Docking Accuracy. *Journal of Medicinal Chemistry* **2004**, *47* (7), 1739–1749. https://doi.org/10.1021/jm0306430.

(18) Porter, N. J.; Mahendran, A.; Breslow, R.; Christianson, D. W. Unusual Zinc-Binding

Mode of HDAC6-Selective Hydroxamate Inhibitors. *Proceedings of the National Academy of Sciences of the United States of America* **2017**, *114* (51), 13459–13464. https://doi.org/10.1073/pnas.1718823114.

(19) Porter, N. J.; Wagner, F. F.; Christianson, D. W. Entropy as a Driver of Selectivity for Inhibitor Binding to Histone Deacetylase 6. *Biochemistry* **2018**, *57* (26), 3916–3924. https://doi.org/10.1021/acs.biochem.8b00367.

(20) Hubbert, C.; Guardiola, A.; Shao, R.; Kawaguchi, Y.; Ito, A.; Nixon, A.; Yoshida, M.; Wang, X. F.; Yao, T. P. HDAC6 Is a Microtubule-Associated Deacetylase. *Nature* **2002**, *417* (6887), 455–458. https://doi.org/10.1038/417455a.

(21) Seto, E.; Yoshida, M. Erasers of Histone Acetylation: The Histone Deacetylase Enzymes. *Cold Spring Harbor Perspectives in Biology* **2014**, *6* (4). https://doi.org/10.1101/cshperspect.a018713.

(22) Venkatesh, P. R.; Goh, E.; Zeng, P.; New, L. S.; Xin, L.; Pasha, M. K.; Sangthongpitag, K.; Yeo, P.; Kantharaj, E. In Vitro Phase I Cytochrome P450 Metabolism, Permeability and Pharmacokinetics of SB639, a Novel Histone Deacetylase Inhibitor in Preclinical Species. *Biological and Pharmaceutical Bulletin* **2007**, *30* (5), 1021–1024. https://doi.org/10.1248/bpb.30.1021.

(23) Rho, H. S.; Baek, H. S.; Lee, J. A.; Park, C. M.; Kim, D. H.; Chang, I. S.; Lee, O. S. Hydroxamic Acid Derivatives and the Preparation Method Thereof, 2009. https://doi.org/WO2005/19162 A1.

(24) Lu, Q.; Yang, Y. T.; Chen, C. S.; Davis, M.; Byrd, J. C.; Etherton, M. R.; Umar, A.; Chen, C. S. Zn2+-Chelating Motif-Tethered Short-Chain Fatty Acids as a Novel Class of Histone Deacetylase Inhibitors, 2004. https://doi.org/10.1021/jm0303655.

(25) London, C. A.; Lin, T.-Y.; Kulp, S. Methods and Compositions for Inhibiting and Preventing the Growth of Malignant Mast Cells, 2011. https://doi.org/WO2011/103563 A1.

Class I/IIb-Selective HDAC Inhibitor Exhibits Oral Bioavailability and Therapeutic Efficacy in Acute Myeloid Leukemia

Andrew E. Shouksmith[†,#], Justyna M. Gawel[†,#], Nabanita Nawar[†], Diana Sina[†], Yasir S. Raouf[†], Shazreh Bukhari[†], Liying He[†], Alexandra E. Johns[†], Pimyupa Manaswiyoungkul[†], Olasunkanmi O. Olaoye[†], Aaron D. Cabral[†], Abootaleb Sedighi[†], Elvin D. de Araujo[†], Patrick T. Gunning[†*]

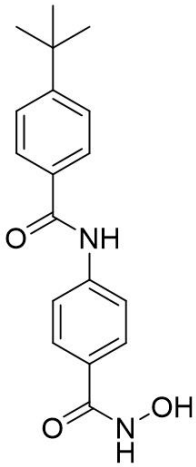

51